Advanced Materials Research Vol. 409 (2012) pp 117-122

doi:10.4028/www.scientific.net/AMR.409.117

On the Interface between Plasma Fluorocarbon Films and 316L Stainless Steel Substrates for Advanced Coated Stents

Maxime Cloutier[a], Stéphane Turgeon[b], Pascale Chevallier[c], Diego Mantovani[d]

Laboratory for Biomaterials and Bioengineering, Department of Min-Met-Materials Engineering, Laval University & University Hospital Research Center, Quebec City, G1V 0A6, Canada

[a]Maxime.Cloutier.2@ulaval.ca, [b]Stephane.Turgeon@crsfa.ulaval.ca, [c]Pascale.Chevallier@crsfa.ulaval.ca, [c]Diego.Mantovani@gmn.ulaval.ca

Keywords: Interface, corrosion resistance, plasma reoxidation, ultra-thin polymer films, oxide layer

Abstract As intravascular biomedical devices, metallic stents are particularly susceptible to corrosion induced by the physiological environment, causing the degradation of mechanical properties and leading to the release of toxic and carcinogenic ions from the SS316L bulk. Therefore, several works have been focused on the development of an ultra-thin fluorocarbon coating that could act both as a drug-carrier for in-stent restenosis and as an anti-corrosion barrier. However, the increase of the corrosion performance was limited by the inevitable permeability of the coating, which exposed some of the sensitive interfacial region to the corrosive environment. Indeed, in previous works, adhesion and growth rate of the film were promoted by the removal of the native oxide layer of the stainless steel which is inhomogeneous, brittle and mechanically unstable. Further refinements of the interface are therefore required in order to enhance the overall corrosion performance without compromising the fluorocarbon film properties and adhesion. Hence, the aim of this work was to enhance the corrosion behaviour of coated SS316L by the creation of a controlled interfacial oxide layer. The native oxide layer was first removed under vacuum and the bare metal surface was subjected to a plasma-reoxidation treatment. Tafel measurements were used to assess the corrosion rates of the specimens. Coated and uncoated modified interfaces were also characterized by X-Ray Photoelectron Spectroscopy (XPS) and Atomic Force Microscopy (AFM).

Introduction

Stents are thin wire mesh tubes, mainly made of 316L stainless steel (SS316L), used to provide internal scaffolding to diseased arteries while preventing the obstruction of blood flow [1]. Chosen for its excellent mechanical properties, essential for biomedical applications, stainless steel is naturally covered with a mixture of iron and chromium oxides, creating a surface layer which is brittle and mechanically unstable under stress [2]. Moreover, due to its exposure to the blood flow, corrosion has been a major issue as degradation of mechanical properties and release of carcinogenic and toxic metallic ions has been observed in implanted stainless steel devices [2, 3]. Therefore, one solution developed to prevent the release of metallic ions was coated and drug-eluting stents [4]. However, poor film adhesion, due to the use of commercial coating techniques, such as coating by spraying or dipping, led to numerous cases of in-stent restenosis, thrombosis, stent fractures and coating failures [5, 6]. In this context, we developed a plasma polymerization process allowing the deposition of ultra-thin fluorocarbon coatings (CF_x) on SS316L since this deposition technique is known to favour film adhesion [7]. CF_x deposition on SS316L has been investigated and previous results showed good adhesion properties and film stability over time. It was shown that the most effective way to promote adhesion and film growth was through the etching of the native oxide layer [7]. However, the oxide layer thinning due to the etching lowered the corrosion resistance of the substrate and affected the stability of the interface. Indeed, despite showing the best adherence and film growth, a tenfold increase in corrosion rate was observed for the completely etched interface. Hence, the corrosion resistance of the coated stainless steel was shown to be inseparable to the interfacial region.

The main objective of this work was to develop an interface with better anti-corrosion properties without degrading the film coverage. Numerous processes have already been studied for the surface modification of SS316L such as, electropolishing, etching, ion implantation, nitriding and heat treatment [8]. However, these procedures are either insufficient for the corrosion protection or detrimental to further plasma polymerization. Hence, we developed a two-step plasma process to enhance the corrosion resistance of the interfacial oxide layer: 1) Complete removal of the native oxide layer through a specific etching process. 2) Exposure of the etched surface to O_2/Ar plasma for the formation of an enhanced anti-corrosion barrier. Then, the samples could be directly coated in the same reactor by pulse-afterglow polymerization. Other reoxidation techniques were also tested. Uncoated and coated samples with different reoxidation processes were subjected to a potentiodynamic test and Tafel measurements were used to assess the corrosion rates of the specimens. Flat samples were also deformed by a small punch test to assess the effects of the stent expansion. The results were compared to those obtained for electropolished samples, a common surface interface treatment for SS316L, and as-received samples, which are mechanically polished. The specimens were also thoroughly characterized by X-Ray Photoelectron Spectroscopy (XPS), Atomic Force Microscopy (AFM).

Experimental

Materials and sample preparation. The PECVD reactor used in this experiment has been previously described in details [9]. Briefly, it consists of a tubular Pyrex chamber capacitively coupled to a radio-frequency generator (13.56 MHz) and pumped by a turbomolecular pump (Varian) with a base pressure of 1 x 10^{-5} mbar. SS316L mechanically polished plates of 500µm thickness (Goodfellow, Devon, PA, USA) were used to punch disks of 12.7 mm diameter. The circular substrates were then cleaned and prepared following a previously described method [9] before entering the reactor. The specimens were treated following two distinct reoxidation procedures and compared with as-received and electropolished substrates. The first step of both processes involved the removal of the native oxide layer by plasma etching. The plasma sequence consisted of a series of C_2F_6 plasma followed by a H_2 plasma repeated eight times (plasma X8), which is explained in details elsewhere [7]. In the second step, the oxide was regrown in the plasma reactor following two different methods. The first reoxidation process was the exposure to a constant O_2 (99,995 % purity) flow for up to 60 minutes, namely controlled reoxidation (CR). In the second procedure, the etched surface was exposed to an oxygen-argon plasma, namely plasma reoxidation (PR). Both methods were optimized by varying the different gas flow rates, ratios and total pressure and treatment time. Polymerization of the CF_x films on the modified interfaces was then carried by pulsed afterglow plasma polymerization in a mixture of C_2F_6 and 6% H_2, with a duty cycle of 20% (t_{on}= 5ms, t_{off}=20 ms) at a pressure of 700 mTorr for 240 s. Details of the optimized interface treatments are summarized in Table 1. Samples were subjected to a 25% plastic deformation using a small-punch test device mounted on a SATEC T20000 testing machine (Instron, Norwood, MA, USA) as previously described [10].

Table 1. Interface treatment parameters

Conditions	Gas flow rate (O_2)	Gas flow rate (Ar)	Gas pressure	Duty cycle	Distance from antenna	Peak Power	Treatment time
Plasma reoxidation	12 sccm	50 sccm	700 mTorr	25% (t_{on} =100ms; t_{off}=300ms)	11 cm	150W	30 min
Controlled reoxidation	12 sccm	-	250 mTorr	-	-		60 min

Corrosion test. The corrosion behaviour was assessed using a 1L three-electrode corrosion cell. A graphite counter –electrode was used as the auxiliary electrode and a saturated calomel electrode as the reference electrode. Measurements were performed with a Model K47 Corrosion Cell system and VersaSTAT 4 Potentiostat controlled by the Versa-Studio software (AMETEK Princeton Applied Research, Oak Ridge, TN, USA). Corrosion measurements were done in aerated Phosphate

Buffered Saline (PBS, Sigma-Aldrich, Oakville, ON, Canada) pH 7.4 heated at ~37°C and under mechanical stirring. The geometric area exposed to the solution was 0,16 cm^2 and 0,32 cm^2 for the non-deformed and deformed samples, respectively. Tafel data were obtained following two steps. First, the Open Circuit Potential (OCP) was monitored for 1 hour after the immersion of the sample. Then, the Tafel plot was scanned by ranging the potential between -250 mV from the OCP and + 1,2 V at a scan rate of 0,167 mV/s. The calculation of the corrosion rate in mm/year is based on Faraday's law $CorrRate = 0.003272 \bullet i_{corr} \bullet (EW / d)$ where 0.003272 is a conversion factor (mm/µA cm year) [11], i_{corr} is the corrosion current density in µA/cm² deduced from Tafel curves, EW is the equivalent weight of SS316L and d is the SS316L density: 25.5g and 8.0 g/cm^3 respectively.

Surface characterization. The surface chemical composition of the CF_x films, modified interfaces and metallic substrates was investigated using an X-ray Photoelectron Spectrometer (XPS - PHI 5600-ci spectrometer, Physical Electronics USA, Chanhassen, MN, USA). Survey spectra were acquired at a detection angle of 45° using the Kα line of a standard aluminum source operated at 300 W. Sputtering for depth analyses was performed with an Ar^+ ion beam of 4 KeV energy and 3 µA/cm^2 current density at an incident angle of 45°. Surface imaging was performed using an Atomic Force Microscope (AFM, Dimension™ 3100, Veeco, Woodbury, NY, USA) operated in Tapping Mode and equipped with an ultra-sharp silicon tip (typical tip radius of 2 nm). Visualization and analysis of the morphology were performed using the WSxM software [12].

Results and discussion

Corrosion resistance. Tafel plots from potentiodynamic tests were used to assess the effectiveness of the reoxidation processes on the corrosion resistance of the sample. For the controlled reoxidation, no effects were observed for the variation of the O_2 flow, pressure and time. This suggests that the oxide layer growth quickly saturates under a gaseous reoxidation process, in accordance with the literature [13]. For the plasma reoxidation, an optimal process was found for an oxygen –argon mixture ratio of 0.2, which was expected to provide the highest rate of oxidation [14]. For all tested samples, CR-treated interfaces showed inferior corrosion resistance when compared to PR-treated samples (Fig. 1). Hence, this process did not seem to exhibit superior anti-corrosion properties and was not studied any further.

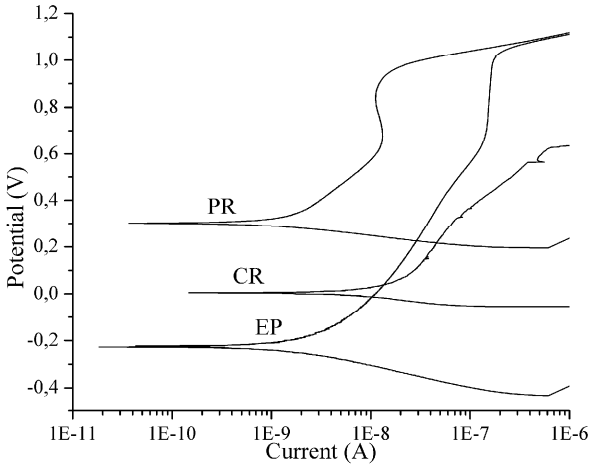

Figure 1. Potentiodynamic polarization curves of uncoated interfaces after electropolishing (EP), controlled reoxidation (CR) and plasma-reoxidation (PR) treatments

Uncoated interfaces showed a marked difference in corrosion rates and potentials before deformation (Table 2). The PR treatment induced a 6-fold reduction in corrosion rate and a + 500 mV increase in corrosion potential over the EP-treated samples. Hence, it displayed the electrochemical behaviour of an appreciably more noble metal, which is a good indication of improved passivity. In general, all samples, other than PR, showed a higher current density and lower corrosion potential over the anodic branch (Fig. 1), indicating inferior resistance to corrosion. This improved thermodynamic stability created by the PR treatment was also assessed for all deformation and coating conditions, as observed in Table 2. As reported in the literature [15-17], the corrosion resistance of SS316L is strongly influenced by the oxide surface properties and the

oxidation process. Thus, the increase observed in the corrosion resistance suggests that PR induced the creation of a thicker oxide layer and/or a lesser defect and porosity density. The role of surface defects in creating active sites for pitting corrosion has been explained by Hashimoto & Asami [15]. Although the uncoated PR interface seemed to crack after the 25% deformation, as observed by the large decrease in corrosion potential, this decrease was not observed for coated PR samples, before and after deformation, therefore showing a marked improvement of the protective behavior of the film, indicative of a lesser defect and porosity density in it also. Moreover, the CF_x-coated PR samples showed the lowest corrosion rate of all deformed samples, making it the most suited condition for stent applications.

Table 2. Corrosion potentials [mV] and rates [μm/year] of samples with different interfaces

		No deformation		25% deformation	
		E_{corr} [mV]	Corrosion rate [μm/year]	E_{corr} [mV]	Corrosion rate [μm/year]
Uncoated	As-received	-162 ± 50	2,1 ± 1,1	-314 ± 35	5,4 ±0,8
	EP	-247 ± 50	0,5 ± 0,3	-307 ± 58	6 ± 2
	PR	285 ± 20	0,082±0,016	-205 ± 33	0,8 ± 0,4
Coated	EP	-231 ± 38	0,6 ± 0,2	-294 ± 13	1,7 ± 0,3
	PR	-28 ± 100	0,091 ± 0,010	-37 ±134	0,2 ± 0,2

Chemical composition. In order to assess the changes induced by the plasma reoxidation process on the thickness and chemical composition of the oxide layer, the interface was studied by XPS depth profiles (Fig. 2). In general, both treatments, EP and PR, exhibited the characteristic surface of SS316L, which is a thin layer composed of chromium and iron oxides. However, Fig. 2b clearly highlights an increase of the oxygen proportion, compared to EP (Fig. 2a), accompanied by a thicker oxide layer induced by plasma reoxidation. Indeed, the thickness measured on the PR-treated surface is 4 times greater than that of the electropolished sample. Moreover, plasma reoxidation produced major modifications of the chromium and iron profiles, resulting in a bi-layered oxide structure (iron rich outer, chromium rich inner), which is not apparent on the electropolished substrate, as illustrated by the Cr/Fe ratio (Fig. 2c). This type of multi-layered structure on stainless steel has already been observed during the formation of oxide layers on stainless steel under controlled conditions [13, 18]. Also, PR being a cold technique, the substrate reached only 85°C during the reoxidation process, it is expected that the PR interface is amorphous, with very little intermetallic phases on the surface [19], as confirmed in Fig. 2b by the low chromium concentration detected on the outer surface. In contrast, the as-received and electropolished surface layers are composed of a mixture of chromium and iron oxides with surface grain boundaries [17, 20]. Grain boundaries are an important source of defects and consequently greatly reduced the corrosion resistance of stainless steel [15, 20]. Additionally, the carbon coverage of the surface in mainly restricted to the topmost layers for both conditions but the PR-treated samples showed less carbon contamination, suggesting a cleaner surface. Finally, fluorine was detected throughout the oxide layer for the PR-treated samples and is due to contamination from the etching X8 process [7].

As already described by Lewis and al. [7], the interface could influence the polymerization process and therefore, the surface composition of coated samples was assessed using XPS (Fig. 3). The F/C ratio was not influenced by the interface treatment, but film oxidation was more pronounced for the EP sample, as highlighted by the tenfold increase in O/C ratios between EP and PR samples. Oxidation is usually related to film stability over time. However, since no ageing process was involved in this study and samples were analyzed under similar conditions, it could be also related to the film coverage of the interface and/or porosity. Indeed, the occurrence of nano-pinholes in the CF_x film has been evidenced before by Hale et al. [21]. The reduction of the oxygen content at the surface of the PR-treated film would then again indicate a more uniform and less porous coating

since there was less exposed interface. Similar observations were made after deformation. This could be attributed to a smoother morphology, but also to the iron-rich outer interfacial layer which is known to be better suited for polymerization [7]. Thus the bi-layer oxide structure formed during PR provides excellent corrosion resistance with a chromium-rich inner layer (Table 2) while presenting iron-rich outer layer beneficial for plasma polymerization.

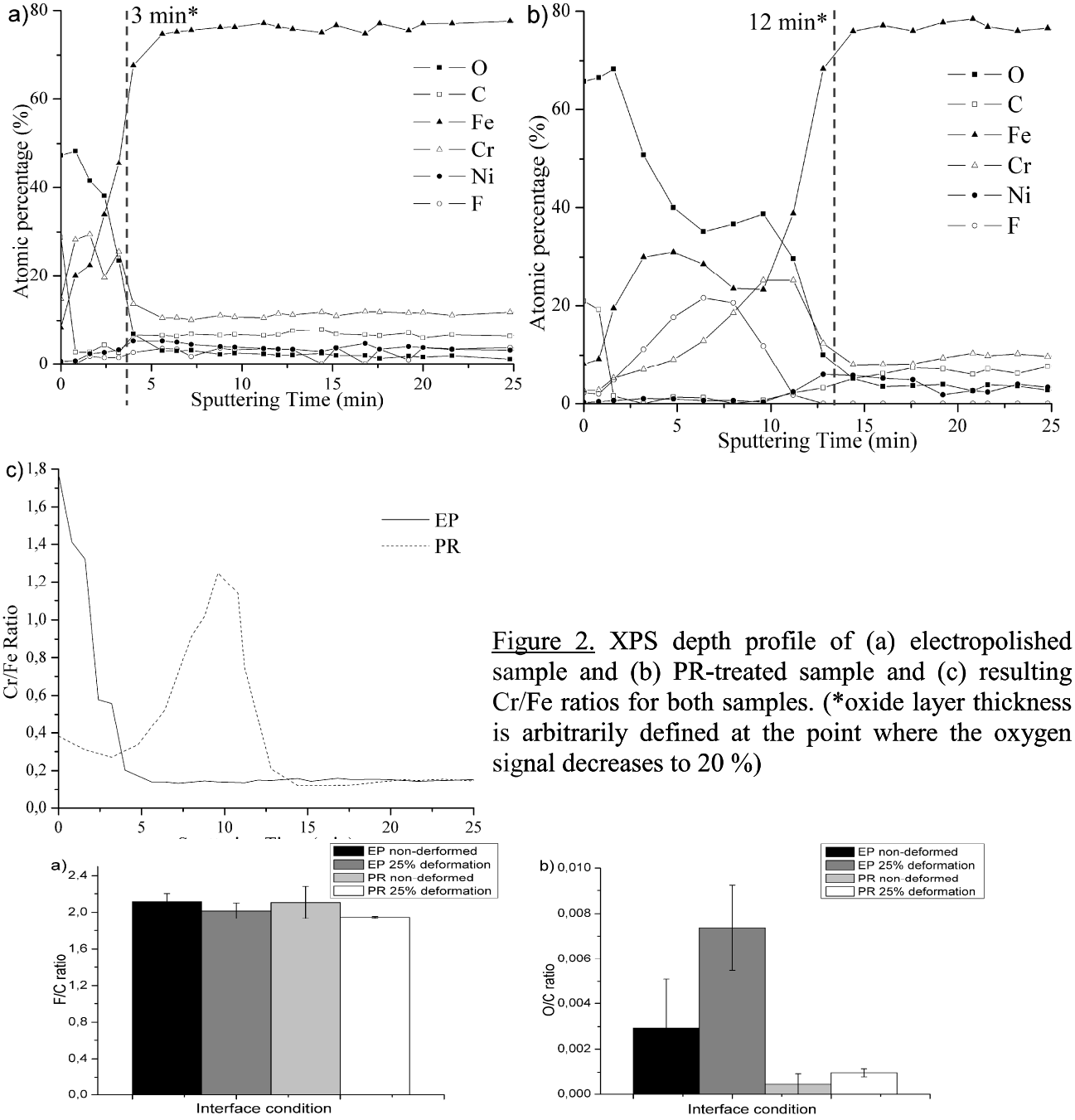

Figure 2. XPS depth profile of (a) electropolished sample and (b) PR-treated sample and (c) resulting Cr/Fe ratios for both samples. (*oxide layer thickness is arbitrarily defined at the point where the oxygen signal decreases to 20 %)

Figure 3. XPS measurements of (a) F/C ratio and (b) O/C ratio of coated EP and PR samples, with and without deformation.

Surface morphology. In order to understand the effects of the interface treatment on the morphology of the oxide layer, the surface was visualized by AFM. EP-treated (R_{RMS}= 6 ± 2 nm) and PR-treated (R_{RMS}= 4,4 ± 1,0 nm) surfaces exhibited a marked improvement of surface smoothness relative to the as-received substrate (R_{RMS}= 100 ± 30 nm), with the latter showing a slightly smoother surface. Roughness parameters were calculated from 20 x 20 μm^2 scans. These results agreed with the potentiodynamic and XPS analyses and suggested that the PR treatment created an interfacial oxide layer with less defects and inhomogeneities. After coating, the PR

samples exhibited films similar to those on the electropolished ones, with similar thickness (~30 nm) and roughness (~5 nm) on both interfaces. The 25 % deformation did not induce any noticeable delamination or cracks in the coating as none were observed on all PR-treated samples (not shown). This suggests a sufficient adhesion of the film as well as cohesion of the interface to resist the stent expansion.

Conclusion

The aim of this work was the development of an interface more resistant to corrosion without degrading the film coverage. After removal of the native oxide layer, plasma reoxidation (PR) gave the most effective anti-corrosion barrier by creating a thick, bi-layered oxide. An iron-rich outer layer allowed superior fluorocarbon polymerization while the chromium-rich inner face and the low surface defects density enhanced the corrosion resistance of the overall sample, as confirmed by Tafel, XPS and AFM analysis. The properties of the PR-treated samples seemed optimal for stent applications. Additional work should be done to investigate directly the amorphous nature of the interface and to lower its fluorine contamination, as it could lead to potential cohesion problems.

Acknowledgements

The authors are grateful to Dr. François Lewis for his previous work on interface modifications and plasma deposition. The authors would also like to thank Dr. Paula Horny and Marie Leroy for their guidance and help in corrosion experiments. This work was supported by the *Natural Sciences and Engineering Research Council* (NSERC), the Canadian Institutes of Health Research, the Fonds Québécois de la Recherche sur la Nature et les Technologies and the Fonds de la Recherche en Santé du Québec. Maxime Cloutier was awarded of an undergraduate student research award granted by the NSERC.

References

[1] H.M. Burt, W.L. Hunter: Adv Drug Deliver Rev Vol. 58 (2006), p. 350
[2] Y. Shaulov, R. Okner, Y. Levi, N. Tal, V. Gutkin, D. Mandler, A.J. Domb: ACS Appl. Mater. Interfaces Vol. 1 (2009), p. 2519
[3] M. Uo, F. Watari, A. Yokoyama, H. Matsuno, T. Kawasaki: Biomaterials Vol. 22 (2001), p. 677
[4] M.J. Eisenberg, K.J. Konnyu: Am J Cardiol Vol. 98 (2006), p. 375
[5] S.H. Lee, J. Park, U. Kim, G. Hong, D. Shin, Y. Kim, B. Shim: Circulation Vol. 114 (2006), p. 394
[6] M. Wiemer, T. Butz, W. Schmidt, K.P. Schmitz, D. Horstkotte, C. Langer: Catheter Cardio Inte Vol. 75 (2010), p. 905
[7] F. Lewis, S. Turgeon, P. Chevallier, J.J. Pireaux, M. Tatoulian, D. Mantovani: Plasma Processes Polym. Vol. 7 (2010), p. 309
[8] *Materials and coatings for medical devices : cardiovascular* (ASM International, Materials Park, OH 2009).
[9] M. Haidopoulos, S. Turgeon, G. Laroche, D. Mantovani: Surf Coat Tech Vol. 197 (2005), p. 278
[10] F. Lewis, D. Mantovani: Macromol. Mater. Eng. Vol. 294 (2009), p. 11
[11] ASTM G102-89: *Standard Practice for Calculation of Corrosion Rates and Related Information from Electrochemical Measurements* (ASTM International, 1994).
[12] I. Horcas, R. Fernández, J.M. Gómez-Rodríguez, J.G.-H. Colchero, J., A.M. Baro: Rev. Sci. Instrum. Vol. 78 (2007), p. 013705
[13] C. Donik, A. Kocijan, D. Mandrino, I. Paulin, M. Jenko, B. Pihlar: Appl Surf Sci Vol. 255 (2009), p. 7056
[14] J. Okado, K. Okada, A. Ishiyama, Y. Setsuhara, K. Takenaka: Surf Coat Tech Vol. 202 (2008), p. 5595
[15] K. Hashimoto, K. Asami: Corrosion Science Vol. 19 (1979), p. 251
[16] R. Singh, N.B. Dahotre: J. Mater. Sci.-Mater. Med. Vol. 18 (2007), p. 725
[17] S.J. Lee, H.J. Lai: J. Mater. Process. Technol. Vol. 140 (2003), p. 206
[18] J.C. Langevoort, I. Sutherland, L.J. Hanekamp, P.J. Gellings: Appl Surf Sci Vol. 28 (1987), p. 167
[19] C.O.A. Olsson, D. Landolt: Electrochim. Acta Vol. 48 (2003), p. 1093
[20] C.-C. Shih, C.-M. Shih, Y.-Y. Su, L.H.J. Su, M.-S. Chang, S.-J. Lin: Corrosion Science Vol. 46 (2004), p. 427
[21] P. Hale, S. Turgeon, P. Horny, F. Lewis, N. Brack, G. Van Riessen, P. Pigram, D. Mantovani: Langmuir Vol. 24 (2008), p. 7897